# IDŐJÁRÁS

*Quarterly Journal of the Hungarian Meteorological Service*
*Vol. 119, No. 1, January – March, 2015, pp. 39–51*

# Radar-based investigation of long-lived thunderstorms in the Carpathian Basin

**Ákos Horváth**[1]*, **András Tamás Seres**[2], and **Péter Németh**[3]

[1]*Hungarian Meteorological Service,*
*Vitorlás u. 17, H-8600 Siófok, Hungary,*
*E-mail: horvath.a@met.hu*

[2]*Hungarian Defence Forces Geoinformation Service,*
*Szilágyi E. fasor 7–9, H-1024 Budapest, Hungary,*
*E-mail: seres.andrastamas@upcmail.hu*

[3]*Hungarian Meteorological Service,*
*Gilice tér , H-1024 Budapest, Hungary,*
*E-mail: nemeth.p@met.hu*

**Corresponding author*

*(Manuscript received in final form April 8, 2014)*

**Abstract** – This study describes a weather-radar-based investigation of long-lived thunderstorms in Hungary in the period of 2004–2012. An objective method was developed for identifying and tracking convective cells. The cells were represented by so-called thunderstorm ellipses. In this research, intensive objects were classified into 3 categories such as severe, highly severe, and extremely severe thunderstorm ellipses. The categories were defined by radar reflectivity thresholds 45 dBZ, 50 dBZ, and 55 dBZ. Only those cells were involved in the investigation whose lifetime extended more than 1 hour. In the 9-year period, 2625 severe, 597 highly severe, and 45 extremely severe long-lived thunderstorm ellipses were found. Stronger cells moved faster and at most intensive cells, right-turning movement was more frequent. Many of these long-lived, strong objects could be supercells. The applied methods and results can be used for severe weather forecast and nowcasting in the Carpathian Basin.

*Key-words:*severe thunderstorm, weather radar, climatology, tracking, supercell, Hungary

## *1. Introduction and background*

Severe thunderstorms and associated phenomena (stormy wind gusts, hailstorms, heavy rainfalls, tornadoes, intensive lightning) often occur in Hungary, mainly in late spring and summer (*Horváth* and *Geresdi,* 2003). These convective storms cause major damages mainly in the electric and transportation networks by wind gusts, in the agriculture by hail storms, and in other branches of the infrastructure by torrential rain and flash floods. A thunderstorm, developed into supercell phase, caused fatal accidents during the Constitution Day firework in Budapest in 2006 (*Horváth et al., 2007*). These events motivate the investigation to overview severe convective cells using 9-year period of observations by radar network of the Hungarian Meteorological Service. In practice, radar reflectivity data are available in that period, what explains why reflectivity based identification and tracking methods were applied for recognizing and tracking intensive thunderstorms.

Radar-based tracking of thunderstorms have been investigated in the United States since the beginning of the 1950's. *Battan* (1952) found that the storm-tops of "longer-lived" (> 20 min) cells were higher than the shorter-lived (≈10 min) ones. *Browning* (1964) defined *the supercell* term for the most organized, most severe, and longest-lived form of isolated, deep moist convection. In 1966, *Wilson* analyzed the relation of thunderstorm size and intensity (*Wilson,* 1966). In the 1970s, the development of remote sensing technique and the surface observations allowed to update the definitions of supercells (*Wilhelmson* and *Klemp*, 1978; *Lemon* and *Doswell*, 1979). Presently, the most accepted theory about supercell thunderstorms was made by *Klemp* (1987). *Henry* (1993) and *MacKeen et al.* (1999) analyzed the relationship between reflectivity–derived storm characteristics and storm longevity. In the last two decades, some radar-based algorithms were developed for tracking thunderstorms *(Lakshmanan* and *Smith*, 2010). The TITAN technique (thunderstorm identification, tracking, analysis and nowcasting) was developed by *Dixon* and *Wiener* (1993), while *Morel et al.* (1997) used a procedure of the extent of overlaps. *Johnson et al.* (1998) applied projected centroid locations and *Han et al.* (2009) combined TITAN and overlap methods.

In Hungary, first investigations of severe convection from dynamical aspects were made in the 1960s (*Bodolainé et al*., 1967; *Götz*, 1968). Later, remote sensing data appeared in the Hungarian studies (*Horváth* and *Práger*, 1985; *Boncz et al.*, 1987). Supercell thunderstorms and formation of tornadoes were described by *Horváth* (1997). Since the 2000s, nowcasting methods (*Horváth* and *Geresdi,* 2003; *Horváth et al.,* 2007; *Csirmaz et al*., 2013) and radar-based thunderstorm climatology (*Horváth et al.,* 2008) have appeared as well.

The aim of this study is to survey incidence and behavior of severe thunderstorms in Hungary using radar observations in the period of 2004–2012 applying radar-reflectivity based recognition and tracking methods.

## *2. Methodology*

Hungary is covered by three weather radars operated by the Hungarian Meteorological Service. These locators work in the western part (near the western end of Lake Balaton on the hill Pogányvár), in the central region (in the southeastern district of Budapest) and in the eastern part (in Nyíregyháza-Napkor) of the country; this system covers most part of the Carpathian Basin. All of them are C-band Doppler radars (wave length=5 cm) (*Geresdi*, 2004) and have been working in operative mode since 2004. During the operative measurement, the Doppler-wind was applied for noise filtering and the results were filtered and smoothed into composite fields. From each scan the highest reflectivity data of the relevant vertical column were chosen and placed into the composite image (*Collier,* 1996). The resolution of the composite PPI (plan position indicator) images was originally 2×2 km in space and 15 minutes in time.

The first step was making a more accurate cell tracking method: the original radar image frequency had to be increased from 15 minutes to 1 minute. The TREC method (tracking radar echoes by correlation) *(Tuttle* and *Foote,* 1990; *Horváth et al.,* 2012) was applied to do the time interpolation. During TREC procedure, correlations were searching between two consecutive radar images, and motion vectors were calculated which describe displacement of radar echoes. The computed motion vector field was used for calculating series of ”artificial” radar images with 1 minute frequency. A brief description of TREC is given in *Appendix A*. For further noise reducing of reflectivity, median-filter method (*Tukey*, 1977) was also applied before beginning the analysis.

The second step was the thunderstorm identification using calculated 1 minute frequency radar reflectivity images. TITAN method developed by *Dixon* and *Wiener* (1993) represents irregular shaped thunderstorms by regular, best fitting ellipses. Parameters of an ellipse can be objectively used to describe the place (by coordinates of ellipses center), the size (by area of ellipses), and even the shape (minor and major axes) of a thunderstorm. The mathematical background of TITAN is given in *Appendix B*. Ellipses calculation of TITAN method expects two types of thresholds as input data: reflectivity limit ($R_{min}$) and area limit ($N_{min}$). $R_{min}$ shows the minimum reflectivity of radar pixels that are involved into ellipse calculation. $N_{min}$ shows the minimum number of pixels whose reflectivity values have to be equal or larger than $R_{min}$, and the strong echoes must form a continuous area. For example: $R_{min}$= 45 dBZ and $N_{min}$=5 mean that the procedure orders ellipses to such thunderstorm cells which have at

least 5 pixels with higher than 45 dBZ reflectivity. These calculated ellipses were named *thunderstorm ellipses* (*Horváth et al*., 2008). An example of cell detecting is shown on *Fig. 1,* where $R_{min}$ is set to 45 dBZ and $N_{min}$=5 pixels. The results can be visualized by the Hungarian Advanced Workstation (HAWK) system (*HMS*, 2012). Note, that the applied radar resolution is 2 km in space, thus $N_{min}$=5 means that the size of a thunderstorm ellipse has to be equal or greater than 20 km$^2$. In the present study, $N_{min}$ was assumed to 5 radar pixels, and 3 different radar reflectivity thresholds were applied: 45, 50, and 55 dBZ. These objects were named *severe*, *highly severe*, and *extremely severe thunderstorm ellipses*, respectively. Using these high reflectivity values, the detected cells could be considered as models of severe thunderstorms and the small or weak convective cells were eliminated.

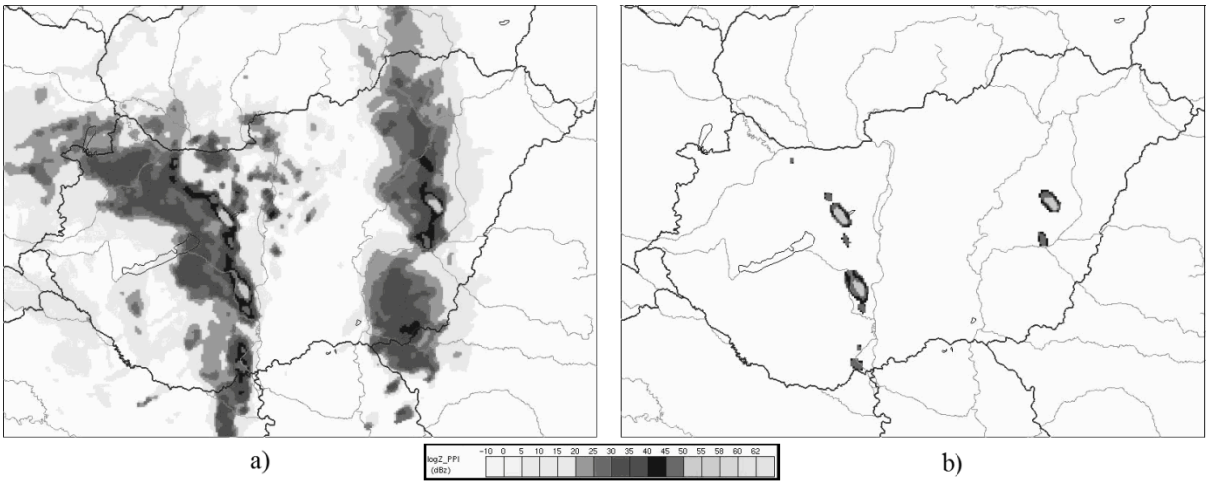


*Fig. 1.* Composite PPI radar images of thunderstorms observed on May 18, 2005, 16:00 UTC: a) original image b) image in which thunderstorms were represented by ellipses. For the visualization, the Hungarian Advanced Workstation (HAWK) system of the Hungarian Meteorological Service was used.

The third step was the cell tracking. For tracking thunderstorm ellipses, a special matching algorithm was applied where position of centrals and area of ellipses were considered to recognize the same cell in the next time step. The algorithm scanned the surrounding area of each ellipsis, and if one or more objects were found on the next image it chose the closest by distance and size. Also distance and size were used to recognize merging, splitting of thunderstorm ellipses. The 1 minute time steps made this procedure fairly reliable: verification on a 50-cell sample showed 98%, comparing with manually tracking. With these methods all information, i. e., size, lifetime, reflectivity, and the track of ellipses were followed and calculated from forming to dissipating and their tracks could be visualized.

The movement of severe thunderstorms, especially supercells, often shows deviation from the straight line, right or left turning of cells are important indicators of supercells (*Lemon* and *Doswell*, 1979). To describe these phenomena, the total deviation angle was introduced. This parameter was calculated in the following way: the displacement of a thunderstorm ellipse in the first 15 minutes designates a direction. Considering the direction coming from the next 15-minute interval, a deviation angle can be calculated. Summing up these angles during the lifetime of the thunderstorm ellipse, the total deviation angle was obtained *(Fig. 2.)*.

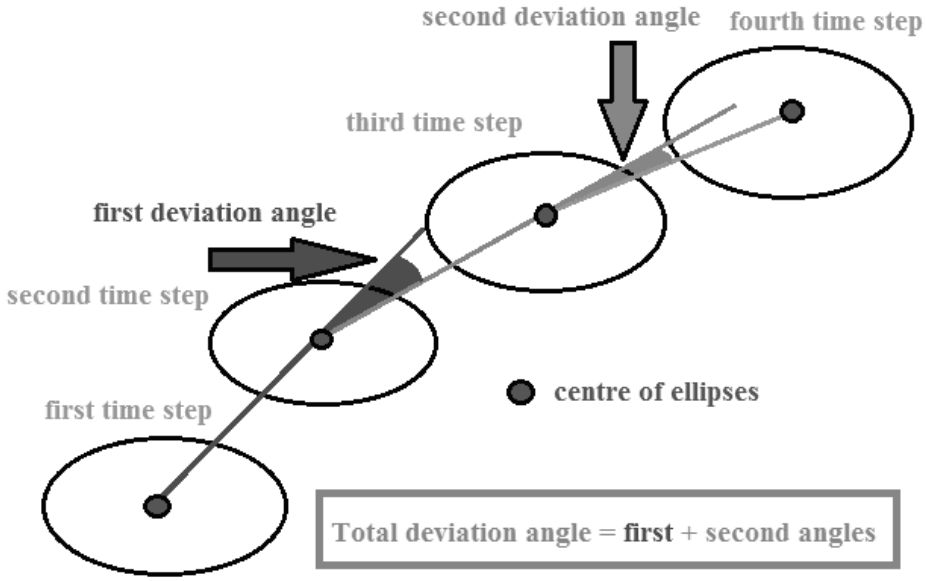


*Fig. 2.* Calculation method of the total deviation angle.

The present study focused on long-lived severe thunderstorms, so the investigation was applied only for severe, highly severe, and extremely severe thunderstorm ellipses with a lifetime more than 1 hour.

## *3. Results*

In the 9-year period, 2625 severe, 597 highly severe, and 45 extremely severe long-lived ellipses were found. *Fig. 3* shows the distribution of lifetime for each type. The maximum of lifetime resolution was around 60 minutes which was followed by rather rapid than moderate decrease in number, and only few severe or highly severe cells lived more than 270 minutes. The average values were 100 minutes for severe, 95 minutes for highly severe, and 86 minutes for extremely severe ellipses.

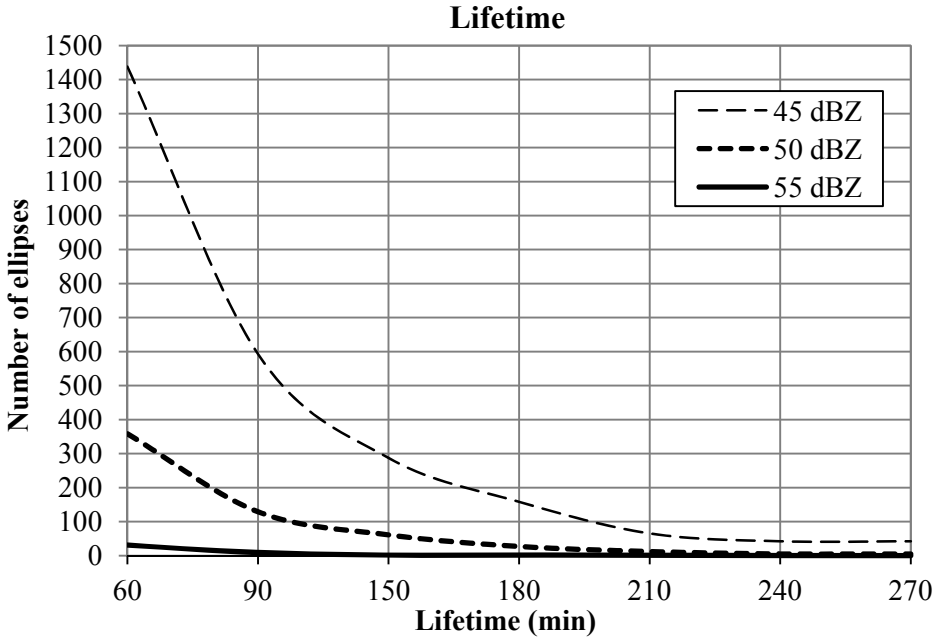


*Fig. 3.* Lifetime characteristics of long-lived severe (45 dBZ), highly severe (50 dBZ), and extremely severe (55 dBZ) ellipses.

The lengths of storm tracks had asymmetric distribution drawing an analogy to log-normal (*Fig. 4*). Most of investigated thunderstorms moved distance between 40 and 80 km during their lifetime and the average distance was about 70 km. There were some cells with extreme long lifetime. For example, on July 14, 2008 a strong cell crossed the whole domain (about 600 km) moving from southwest to northeast.

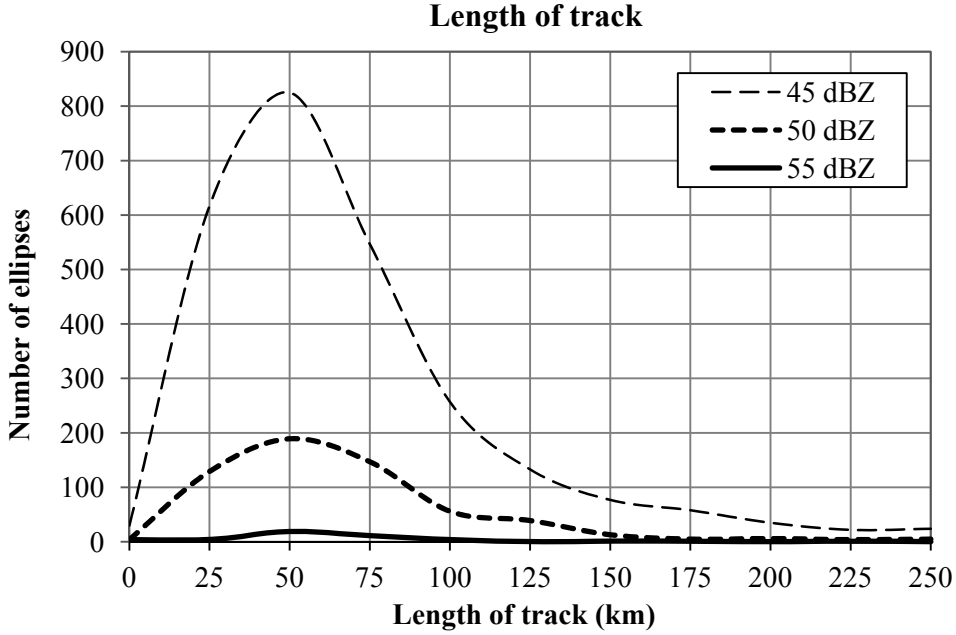


*Fig. 4.* Distribution of storm tracks' length for long-lived severe (45 dBZ), highly severe (50 dBZ), and extremely severe (55 dBZ) ellipses.

The total deviation angle was also investigated. The distribution of total deviation angles was mostly symmetric, especially for ellipses with 45 or 50 dBZ. The ratios between right and left directions were about 50–50% for severe, and 51–49% for highly severe thunderstorm ellipses. At extremely severe thunderstorms this rate was 58–42%, so for most intensive objects, right-turning movement occurred somewhat more often (*Fig. 5*). Considering all investigated thunderstorms, 23% have deviation angle larger than 40° and 13% have larger than 60 degrees.

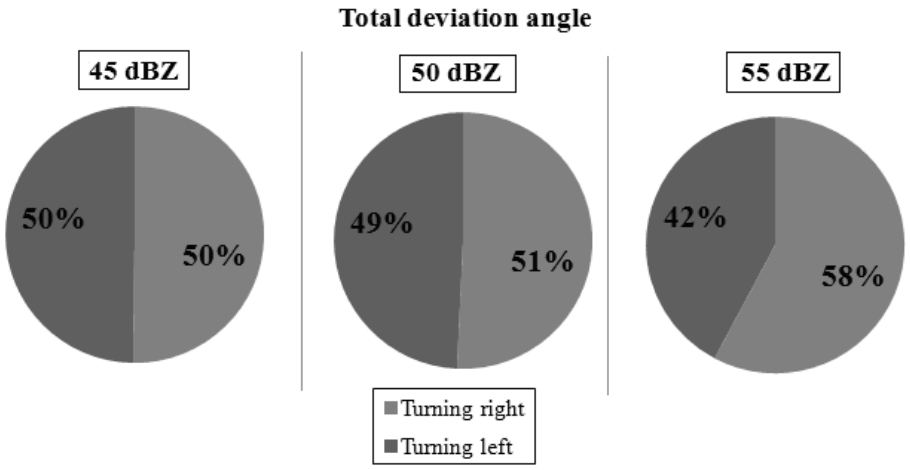


*Fig. 5.* Ratios between positive and negative deviation angles for severe (45 dBZ), highly severe (50 dBZ), and extremely severe (55 dBZ) ellipses.

Knowing lengths of tracks and lifetimes of thunderstorm-ellipses, their average speed could be calculated as well. The distributions of speed were asymmetric: the maximum was around 35–45 km/h (*Fig. 6*). Stronger cells moved faster. For severe thunderstorm ellipses the average speed was 42 km/h, for highly severe objects it was 45 km/h, and for extremely severe ellipses 49 km/h were calculated. Only few (8) severe objects' speed was higher than 100 km/h.

Numbers of severe thunderstorms had wide variability during 9 years. The highest values were in 2010 (with 611 severe, 146 highly severe, and 14 extremely severe ellipses). The lowest numbers were detected in 2005 (with only 95 severe, 13 highly severe, and 0 extremely severe objects).

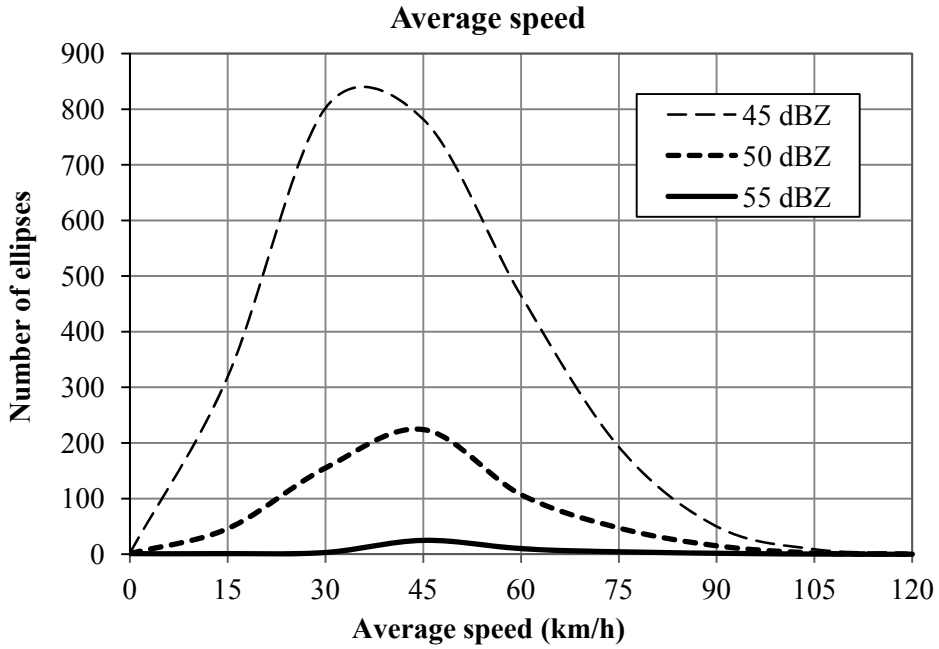


*Fig. 6.* Distribution of average speed for severe (45 dBZ), highly severe (50 dBZ), and extremely severe (55 dBZ) ellipses.

## *4. Conclusions*

This study described a radar-based climatology of long-lived thunderstorms in Hungary focusing on cell motion and tracking in the period of 2004–2012. In our research, intensive thunderstorms were represented with ellipses calculated by the TITAN identification method. During the investigation, severe, highly severe and extremely severe thunderstorm ellipses were distinguished using thresholds of 45 dBZ, 50 dBZ, and 55 dBZ. The investigation was restricted only to thunderstorm ellipses with lifetime exceeded 1 hour.

In the 9-year period, 2625 severe, 597 highly severe, and 45 extremely severe long-lived ellipses were found. The time resolution of thunderstorms during this 9-year period was rather changeable showing the role of larger, synoptic-scale phenomena that determinate condition of the convection. The average values of lifetime were 100 minutes for severe, 95 minutes for highly severe, and 86 minutes for extremely severe ellipses. These values are promising from nowcasting point of view, because cell tracking is a relative easy technique, and persistent cells can be forecasted by extrapolation more than an hour ahead. Lengths of tracks were mostly between 40 and 80 km. Supposing that these storms are able to cause hail and wind damages, there is a high probability that populated places, sensitive infrastructure, or industrial areas were hit by the investigated storms. Stronger cells moved faster, the average speeds were 42 km/h for severe, 45 km/h for highly severe, and 49 km/h for

extremely severe objects. At most intensive cells, right-turning movements were more frequent. At 23% of thunderstorms, significant deviations from the straight line (>40°) were found. These deviations suggest existence of supercells. Considering the 23% of 2625 detected thunderstorms in 9 years*, the estimated number of supercells in a year is 67*.

These results are parts of the work dealing with severe storm climatology. Further researches are needed involving surface observations to obtain wind, pressure, and precipitation fields associated with thunderstorms, and more NWP case studies should be used for understanding the mechanism of severe convective storms in the Carpathian Basin.

***Acknowledgement:*** This study is related to COST-0905 project.

## *References*

*Battan, L.J.,* 1952: Formation of precipitation in natural clouds indicated by radar. Preprints, Third Conference on Radar Meteorology, Montreal, PQ, Canada, Amer. Meteor. Soc., A9–A16.

*Bodolainé, J.E., Bodolai, I.* and *Böjti, B.,* 1967: Macrosynoptical conditions for the formation of Slovenenian squall lines and some properties of cold fronts with thunderstorm. *Időjárás 67*, 129–143.

*Boncz, J., Kapovits, A., Pintér, F.* and *Tänczer, T.*, 1987: A method for the complex analysis of synoptic weather radar and satellite data. *Időjárás 91*, 11–22.

*Browning, K. A.*, 1964: Airflow and precipitation trajectories within severe local storms which travel to the right of the winds. *J. Atmos. Sci. 21*, 634–639.

*Collier, C.G.,* 1996: Application of weather radar system: A Guide to uses of radar in meteorology and hydrology. John Wiley & Sons.

*Csirmaz, K., Simon, A., Pistotnik, G., Polyánszky, Z., Neštiak, M., Nagykovácsi, Zs.* and *Sokol, A.,* 2013: A study of rotation in thunderstorms in a weakly- or moderately-sheared environment. *Atmos. Res. 123,* 93–116.

*Dixon, M.,* and *Wiener, G.,* 1993: TITAN: Thunderstorm Identification, Tracking, Analysis and Nowcasting—A radar-based methodology. *J. Atmos. Oceanic Technol. 10*, 785–797.

*Doviak, R.J.* and *Zrinic, D.S.*, 1993: Doppler Radar and Weather Observations. Academic Press, 335–340.

*Geresdi, I.,* 2004: Felhőfizika. Dialóg Campus, Budapest, 153–170. (in Hungarian)

*Götz, G.,* 1968: Hydrodynamic relationships between heavy convection and the jet stream. *Időjárás 72*, 157–165.

*Han,* L.*,* S. *Fu,* L. *Zhao,* Y. *Zheng,* H. *Wang,* and *Lin, Y.*, 2009: 3D convective storm identification, tracking and forecasting–An enhanced TITAN algorithm. *J. Atmos. Oceanic Technol. 26*, 719–732.

*Henry, S.G.*, 1993: Analysis of thunderstorm lifetime as a function of size and intensity. Preprints, 26th Conf. on Radar Meteorology, Norman, OK, Amer. Meteor. Soc., 138–140.

*Horváth, Á.*,1997: Tornado. *Légkör 62,* 2–9. (in Hungarian)

*Horváth, Á.* and *Práger, T.*, 1985: Zivatarláncok dinamikája és előrejelezhetőségét. *Időjárás 89*, 141–160. (in Hungarian)

*Horváth, Á.* and *Geresdi, I.,* 2003: Severe storms and nowcasting in the Carpathian Basin. *Atmos. Res. 67–68,* 319–332.

*Horváth, Á., Ács, F.* and *Seres, A. T.,* 2008: Thunderstorm climatology analyses in Hungary using radar observations. *Időjárás 112,* 1–13.

*Horváth, Á., Seres, A.T.* and *Németh, P.*, 2012: Convective systems and periods with large precipitation in Hungary. *Időjárás 116*, 77–91.

*Horváth, Á., Geresdi, I., Németh, P.* and *Dombai, F.*, 2007: The Constitution Day storm in Budapest: Case study of the August 20, 2006 severe storm. *Időjárás 111,* 41–65.

*HMS, Hungarian Meteorological Service,* 2012: HAWK-3 visualization system. http://www.met.hu/en/omsz/tevekenysegek/hawk/

*Johnson,* J., P. *MacKeen,* A. *Witt,* E. *Mitchell,* G. *Stumpf,* M. *Eilts,* and *Thomas*, *K.*, 1998: The Storm Cell Identification and Tracking algorithm: An enhanced WSR-88D algorithm. *Weather Forecast 13*, 263–276.

*Klemp, J.B.,* 1987: Dynamics of tornadic thunderstorms. *Ann. Rev. Fluid Mech. 19,* 369–402.

*Lakshmanan, V*. and *Smith, T.,* 2010: An Objective Method of Evaluating and Devising Storm-Tracking Algorithms. *Weather Forecast. 25*, 701–709.

*Lemon, L. R*. and *Doswell III, C. A.,* 1979: Severe thunderstorm evolution and mesocyclone structure as related to tornadogenesis. *Mon. Weather Rev. 107,* 1184–1197.

*MacKeen, P.L., Brooks, H.E.* and *Elmore, K.L.*, 1999: Radar Reflectivity–Derived Thunderstorm Parameters Applied to Storm Longevity Forecasting. *Weather Forecast. 14,* 289–295

*Morel,* C.*, Orain, F.,* and *Senesi, S.,* 1997: Automated detection and characterization of MCS using the Meteosat infrared channel. Proc. Meteorological Satellite Data Users Conf., Brussels, Belgium, EUMETSAT, 213–220.

*Tukey, J.W*., 1977: Exploratory Data Analysis. Addison-Wesley, Reading, 688. pp.

*Tuttle, J.D.* and *Foote, B.,* 1990: Determination of the Boundary Layer Airflow from Single Doppler Radar. *J.Atmos. Ocean. Tech. 7,* 218–232.

*Wilhelmson, R.B.* and *Klemp J.B.,* 1978: A numericalsStudy of storm splitting that leads to long-lived storms. *J. Atmos. Sci. 35*, 1974–1986.

*Wilson, J.W.,* 1966: Movement and predictability of radar echoes. Tech. Memo IERTM-NSSL-28, National Severe Storms Laboratory.

## *Appendix A*

### *Calculation of motion vectors using time series of radar reflectivity*

(*Tuttle* and *Foote*, 1990; *Horváth et al*., 2012)

In the period of 2004–2012, the Hungarian radar network collected data in 15-minute cycles. For a more accurate cell tracking procedure, the original radar image frequency had to be increased using the correlation tracking method TREC (tracking radar echoes by correlation; *Tuttle* and *Foote*, 1990). During the TREC procedure, the radar grid was divided into so-called macro grids, and the calculation of motion vectors was based on maximum correlations for the macro grids. After quality control to filter out noisy vectors on macro grids, fine resolution motion vectors were interpolated for all grid points of the original radar grid. Once a motion vector field – belonging to radar images at time T2 and T1 – is available, interpolation of the radar reflectivity can be done at any time between T1 and T2. Echoes from T1 are moved forward and echoes from T2 moved backward by motion vectors, and the reflectivity of a given pixel is interpolated between the forward and backward moving reflectivity values as shown in *Fig. 7.*

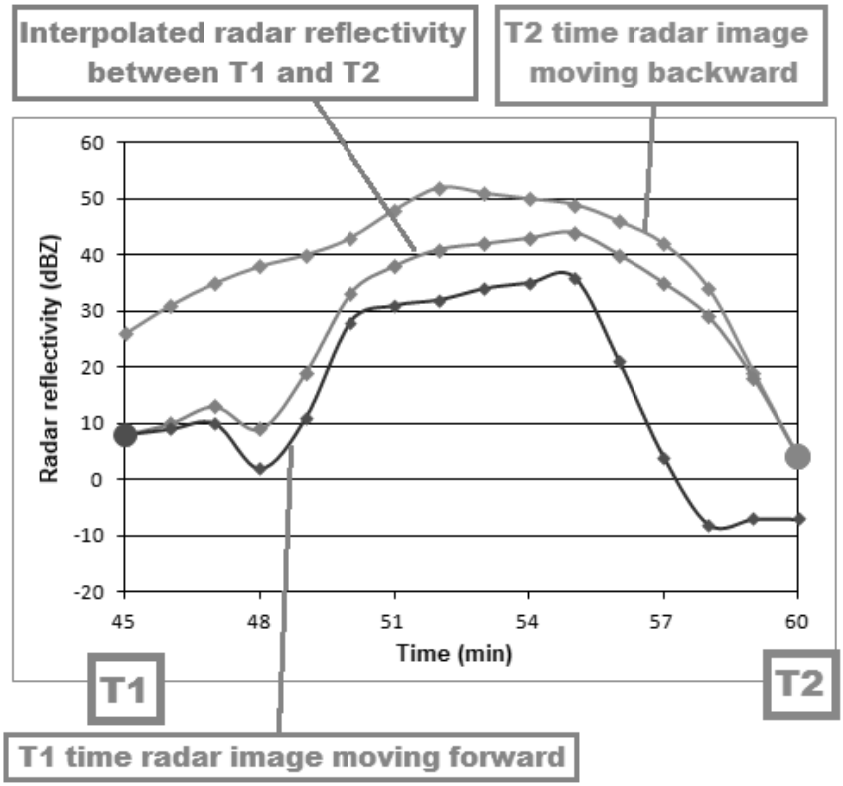


*Fig. 7.* Interpolation of radar reflectivity using motion vectors.

The application of the TREC method offers a more realistic and accurate cell tracking procedure. The optimal interpolation time step for calculation was found to be 1 minute.

## *Appendix B*

### *Mathematical background of the identification*

(*Dixon* and *Wiener*, 1993)

Suppose there is an irregular cluster on a radar image which has $n$ detected pixels. The center of a cluster is defined by

$$\bar{x} = \frac{1}{n}\sum_{i=1}^{n} x_i , \qquad \bar{y} = \frac{1}{n}\sum_{i=1}^{n} y_i , \tag{1}$$

where $x$ and $y$ indicate the longitude and latitude of pixels which have reflectivity higher than a given threshold value. The covariance matrix of this cluster is

$$A = \mathrm{cov}_{xy} = \begin{bmatrix} d & e \\ e & f \end{bmatrix}, \tag{2}$$

where $d$ is the deviation from the center by the $x$ coordinate

$$d = \frac{1}{n-1}\sum_{i=1}^{n}(x_i - \bar{x})^2, \tag{3}$$

f is the deviation from the center by the y coordinate

$$f = \frac{1}{n-1}\sum_{i=1}^{n}(y_i - \bar{y})^2, \tag{4}$$

and $e$ is

$$e = \frac{1}{n-1}\sum_{i=1}^{n}(x_i - \bar{x})(y_i - \bar{y}) . \tag{5}$$

The eigenvalues of the covariance matrix are given by

$$\lambda_1, \lambda_2 = \frac{(d+f) \pm \left[(d+f)^2 - 4(df - e^2)\right]^{1/2}}{2}. \tag{6}$$

The normalized eigenvectors of this matrix are

$$\nu = \left[\frac{1}{(1+g)^2}\right]^{1/2} \qquad \mu = -g\nu, \tag{7}$$

where

$$g = \frac{f + e - \lambda_1}{d + e - \lambda_2}. \tag{8}$$

Then the rotation of the ellipse major axis relative to the $x$ axis is given by these vectors

$$\theta = \tan^{-1}\left(\frac{\nu}{\mu}\right). \tag{9}$$

The eigenvalues of the covariance matrix *($\lambda_1$* and *$\lambda_2$)* represent the variances of the data (pixels)

$$\sigma_{major} = \lambda_1^{1/2}, \qquad \sigma_{\min or} = \lambda_2^{1/2}. \tag{10}$$

The area of the detected cluster is

$$A = ndxdy \tag{11}$$

where *dx* and *dy* are the grid spacing on the radar image. The area of an ellipse is given by

$$T = \pi\, ab, \tag{12}$$

where *a* and *b* represents the major and minor axes of the ellipses.
The main idea is that the area of the irregular cluster and the area of the ellipse have to be equal, therefore

$$A = T. \tag{13}$$

So the major and minor axes of the ellipses can be calculated by

$$a = \sigma_{major}\left(\frac{A}{\pi\sigma_{\min or}\sigma_{major}}\right)^{1/2}, \quad b = \sigma_{\min or}\left(\frac{A}{\pi\sigma_{\min or}\sigma_{major}}\right)^{1/2}. \tag{14}$$

With these parameters *($\bar{x}, \bar{y}$, a, b, $\theta$)*, the focus points and the equation of the ellipse can be determined.